ELSEVIER

Cryogenics 41 (2001) 49–57

Cryogenics

www.elsevier.com/locate/cryogenics

Computational study of a 4 K two-stage pulse tube cooler with mixed Eulerian–Lagrangian method

Y.L. Ju *,1

Cryogenic Laboratory, Chinese Academy of Sciences, P.O. Box 2711, Beijing 100080, People's Republic of China

Received 1 December 2000; accepted 5 March 2001

Abstract

A new mixed Eulerian–Lagrangian numerical model for simulating and visualizing the internal processes and the variations of dynamic parameters of a two-stage pulse tube cooler (PTC) operating at 4 K temperature region has been developed. We use the Lagrangian method, a moving grid, to follow the exact tracks of gas particles as they move with pressure oscillation in the pulse tube to avoid any numerical false diffusion. The Eulerian approach, a fixed computational grid, is used to simulate the variations of dynamic parameters in the regenerator. A variety of physical factors, such as real thermal properties of helium, multi-layered magnetic regenerative materials, pressure drop and heat transfer in the regenerator, and heat exchangers, are taken into account in this model. The time-variations of gas temperature, pressure, mass flow rate, enthalpy flow in a cycle, in first- and second-stage regenerators are presented in the paper. More attention is paid to the effects of different regenerative materials on the performance of the 4 K two-stage PTC.

Keywords: 4 K-pulse tube cooler; Two-stage; Computational study

1. Introduction

The growing need for cryogenic cooling of MRI magnets, SQUIDs and the associated superconducting devices has brought about a strong demand for high reliability and efficiency in coolers. In recent years there have been many developments and improvements in pulse tube coolers (PTCs) [1,2]. Recently multi-stage 4 K PTCs [3–5] have been reported with multi-layered hybrid magnetic materials in the coldest regenerator region. Two-stage PTCs can provide more than 0.5 W cooling power at 4.2 K and meet cooling the requirements of superconducting devices operating at 4 K [6]. By using ^{3}He as the working fluid, the lowest temperature below 1.8 K has been achieved [7]. However, there are still some urgent problems that retard the performance (cooling power, COP, etc.) of 4 K PTCs which are not well understood. For example, the effects of the salient characteristics of real thermal properties of helium, the unique features of physical properties of magnetic regenerator material, and the existence of helium in the void space of the regenerator on the performance of PTCs. They are very difficult to evaluate only by experimental investigation.

Theoretical analysis is critically important to understand the dynamic characteristics and internal processes in PTCs. A numerical method of a two-stage PTC developed by Wang [8,9] was used for designing their 4 K regenerator and revealed several unique features that were different from a conventional single-stage regenerator. However, in his model he (1) neglected the thermal conductivity of the gas and the regenerative materials, which has some unique effects on the pronounced temperature gradient [10], (2) neglected the pressure drop in the regenerator, and (3) focused only on the second-stage regenerator and the pulse tube, and neglected the interaction between the first- and the second-stage regenerators and the pulse tubes.

Eulerian methods have been adopted very broadly and found to be useful for simulating this problem [8,9,11,12]. In such methods the grids are fixed. They solve the fluid variables on fixed grids and reconstruct the interface of gas particles based on the fluid fraction

* Tel.: +86-10-6262-7302; fax: +86-10-6256-4049.
E-mail address: yonglin@cl.cryo.ac.cn (Y.L. Ju).
[1] On leave from Faculty of Applied Physics, Eindhoven University of Technology, P.O. Box 513, NL-5600 MB Eindhoven, The Netherlands.

0011-2275/01/$ - see front matter
PII: S0011-2275(01)00047-9

Nomenclature

A	area (m^2)
C_P	specific heat of helium gas (J/K kg)
C_r	specific heat of buck regenerator material (J/K kg)
D_h	hydraulic diameter of regenerator material (m)
f	filling factor
F	heat exchange area per unit volume (m^2/m^3)
G	atomic mass of helium gas (g/mol)
h	specific enthalpy (J/kg)
H	enthalpy (J)
l	distance of the gas traveling (m)
L	length (m)
m	mass flow rate (g/s)
N	number of moles in subsystem (mol)
n	molar flow rate (mol/s)
p	pressure (Pa)
Pr	Prandtl number
Q	heat (J)
R	ideal gas constant (J/K kg)
Re	Reynolds number
t	time (s)
T	temperature (K)
u	velocity (m/s)
V	volume (m^3)
V_m	specific volume of gas (m^3/kg)
W	work (J)
x	axial length coordinate (m)
z_r	flow impedance factor (m^{-2})
Z_r	flow impedance (m^{-3})

Greeks

α	heat transfer coefficient (W/K m^3)
α_V	volumetric thermal expansion coefficient (K^{-1})
ρ	gas density (kg/m^3)
η	viscosity (sPa)
κ	thermal conductivity (W/K m)
κ_T	isothermal compression coefficient (Pa^{-1})
γ	ratio of heat capacity for ideal gas, C_P/C_V
ξ	ratio of specific heat capacity, Eq. (31)
ω	angular frequency (s^{-1})

Subscripts

0	average
1	orifice
2	double-inlet
b	buffer
c	cold end
fi	left boundary of the sub-system i
g	gas
h	hot end
i	sub-system
m	Molar quantity
o	orifice
r	regenerator matrix materials
t	pulse tube

data in each node. In order to obtain the interfaces accurately, highly refined grids are required for sharp variations of thermal properties. The advantages of Eulerian approach are that employing fixed grids affords simplicity and availability of well-tested, economical field solvers. However, it is not suitable when details of the gas particles are to be explicitly tracked since the interface is reconstructed from the distribution of certain computed field variables. The main drawback of the Eulerian method is that it may bring numerical false diffusion since additional field variables are introduced to model the presence of a moving discontinuity on the computational grid.

In this paper a new mixed Eulerian–Lagrangian numerical model for simulating the variations of dynamic parameters of a 4 K two-stage pulse tube has been developed. We use the Lagrangian method, a moving grid, to follow the tracks of gas particles as they move with pressure oscillation in the pulse tube to avoid any numerical false diffusion. The Eulerian approach, a fixed computational grid, is used to simulate the dynamic parameters in the regenerator. The Lagrangian component of the present model allows tracking accurately the gas particles in the pulse tube. This is a significant improvement over the conventional Eulerian methods. A variety of physical factors, such as real thermal properties of helium, multi-layered magnetic regenerative material, pressure drop and heat transfer in the regenerators, and heat exchangers, are taken into account. We will give, in this paper, the numerical model and some predicted results of time variations of dynamic parameters in a cycle, in the first- and second-stage regenerators. We also pay attention to the effects of different regenerative materials on the performance of the cooler.

2. Physical model and governing equations

Fig. 1 shows the schematic design of a two-stage PTC, which includes compressor, aftercooler, regenerator, cold-end heat exchanger, pulse tube, hot-end heat exchanger, orifice, buffer, and double-inlet valve. In the present study, if the double-inlet valves 10 and 17 are closed, the model is a conventional orifice pulse tube. A one-dimensional model, neglecting any geometric complexity in the regenerator, has been adopted to reduce the CPU time and avoid any difficulty involved with the two- or three-dimensional models. Other basic assumptions are as follows:

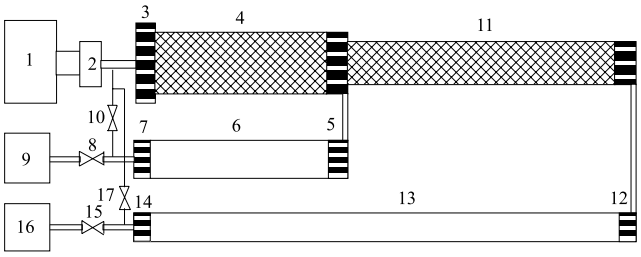

Fig. 1. Schematic design of two-stage PTC. 1 – Compressor; 2 – rotary valve; 3 – aftercooler; 4, 11 – regenerator; 5, 12 – cold end; 6, 13 – pulse tube; 7, 14 – hot-end heat exchanger; 8, 15 – orifice valves; 9, 16 – buffers; 10, 17 – double-inlet valves.

1. The gas flow is laminar, no turbulence.
2. Constant wall temperature at the cold- and hot-end heat exchangers.
3. The regenerative material in the regenerator is incompressible, uniform porosity.
4. Boundary and variable permeability effects are neglected.
5. The pressure drop in pulse tube is neglected.

On the bases of these assumptions, a set of differential equations for a small sub-system ($\Delta x \to 0$), can be expressed as follows (for simplicity the subscript 'g' for the gas is omitted):

Continuity equation

$$\frac{\partial \rho}{\partial t} + \frac{\partial \rho u}{\partial x} = 0. \tag{1}$$

Energy equation of the gas

$$(1-f)\rho \frac{\partial H}{\partial t} = -\rho u \frac{\partial H}{\partial x} + (1-f)\frac{\partial p}{\partial t} + \alpha F(T_r - T) + \frac{\partial}{\partial x}\left(\kappa \frac{\partial T}{\partial x}\right). \tag{2}$$

For real gas the enthalpy H treated as a function of gas temperature T and pressure p can be expressed as

$$\mathrm{d}H = C_P \,\mathrm{d}T + \left\{1 - \frac{T}{V_m}\left(\frac{\partial V_m}{\partial T}\right)_P\right\} V_m \,\mathrm{d}p = C_P \,\mathrm{d}T + (1 - T\alpha_V) V_m \,\mathrm{d}p. \tag{3}$$

Substituting Eq. (3) into Eq. (2) one can find

$$(1-f)\rho C_P \frac{\partial T}{\partial t} = -\rho C_P u \frac{\partial T}{\partial x} - u(1 - T\alpha_V)\frac{\partial p}{\partial x} + (1-f)T\alpha_V \frac{\partial p}{\partial t} + \alpha F(T_r - T) + \frac{\partial}{\partial x}\left(\kappa \frac{\partial T}{\partial x}\right). \tag{4}$$

Energy equation of the matrix in regenerator

$$f\rho_r C_r \frac{\partial T_r}{\partial t} = \alpha F(T - T_r) + \frac{\partial}{\partial x}\left(\kappa_r \frac{\partial T_r}{\partial x}\right). \tag{5}$$

Pressure drop of the gas (in first order)

$$\frac{\partial p}{\partial x} = -\eta z_r u. \tag{6}$$

Equation of state for real gas

$$\rho = f(T, p). \tag{7}$$

The gas velocity here is defined as

$$u = \frac{m}{(1-f)\rho A_r},$$

where m is the mass flow rate and A_r the cross-sectional area of the regenerator. The forms of above equations are given by mass quantity, they can be written based on molar quantity as well. For example the molar flow rate $n = m/G$, where G is the atomic mass of helium gas.

The heat transfer coefficient α of the regenerator is calculated by the correlation equations given in [11]:

$$\alpha = 0.023 \frac{\kappa}{D_h} Re^{0.8} Pr^{0.4}. \tag{8}$$

Here

$$Re = \frac{\rho u D_h}{\eta}. \tag{9}$$

The flow impedance factor z_r of the regenerator is determined by the experimental data [13] and used in [10,14]. Here we take $z_r = 31 \times 10^9\ \mathrm{m}^{-2}$.

It should be noted that the mass flow rate is defined as positive if the gas flows from the compressor to the buffers and as negative for the opposite flow. We assume constant (room) temperature in the compressor that is the left boundary. The inlet gas temperature at the left boundary is given as follows:

$$T_1 = T_{in} = \text{const} \quad m_{in} \geqslant 0, \tag{10}$$

$$T_1 = T_{gas} \quad m_{in} \leqslant 0. \tag{11}$$

The right boundary in the simulation is the buffer, where the gas is regarded as isothermal. It is reasonable to assume constant wall temperature at the hot and cold ends of heat exchangers

$$T_{ci} = T_{c0} = \text{const}, \tag{12}$$

$$T_{hi} = T_{h0} = \text{const}. \tag{13}$$

The initial pressure variations inside the pulse tube are assumed as harmonic variations

$$p = p_0 + p_1 \sin \omega t. \tag{14}$$

It will be modified from the pressure differences in the regenerator system. Both the orifice and double-inlet valves are considered as a resistance component. The mass flow rates through these valves are determined from the pressure differences [14]

$$m_1 = \frac{p_t - p_b}{\eta Z_1}\frac{p_b}{RT_b}. \tag{15}$$

Here $Z_1 = z_1(\Delta x/A_1)$ is the flow impedance of the valves which was determined by the experimental data [13].

3. Numerical methods

Eqs. (1), (4)–(6) with boundary conditions make up the set of governing equations, which is used for determining four independent variables of the gas temperatures T, the matrix temperature T_r, the gas velocity u, and the gas pressure p. They are non-linear and unsteady, and can only be solved by numerical integration.

To solve these equations a combination of the Eulerian and Lagrangian approaches has been developed. We use the conventional Eulerian method, a fixed computational grid, to simulate the variations of dynamic parameters in the regenerator. The Lagrangian approach, a moving grid, is used to follow the tracks of gas particles as they move with pressure oscillation in the pulse tube to avoid any numerical false diffusion.

3.1. Eulerian method

The numerical simulation of the governing equations by Eulerian method is based on the finite difference methodology. The regenerator is divided into many subsystems and each subsystem is considered as a uniform system which can exchange heat and mass with the surroundings through its boundaries. The regenerator domain discretization is made using a control volume approach by inter-nodal method as described by Patankar [15]. Eqs. (1), (4)–(6) are solved by using the explicit scheme, thus the temperature, velocity and pressure are updated in an explicit fashion. Spatial derivatives are approximated using a upwind second-order difference formula, whose construction has been discussed in [11,12], to ensure the transportive properties of the discretization equations. The interface of gas particles is advanced in time by the Lagrangian translation of the gas particles (as discussed below). While the normal mass flow rate is computed from the mass conservation equation (1).

The physical problems discussed here are strongly affected by viscous effects and thermal diffusion effects, to enforce the continuity constraint, the mass conservation over a control subsystem volume is used to update the mass flow rate and the pressure field. Additional details regarding the numerical simulation and procedures are given in [11,12], to reduce CPU time and increase the calculation accuracy.

A solution is obtained from an initial guess (for example, linear temperature profile and harmonic pressure variations) through an iterative scheme using a line-by-line tridiagonal matrix algorithm (TDMA) method. The iteration results should be satisfied by the periodic stable conditions for all the time-dependent parameter and the energy balance condition for the regenerator matrix over one cycle. After a grid refinement study, all calculations presented below are carried out using a 200 uniform grid size. Owning to the explicit nature of the scheme, the time step is restricted by the convective Courant–Friedrichs–Lewy (CFL) limitations, which is set to ~0.0055 s (time period/180). With the space size and time step selected in numerical study, our experiences indicated that the calculated results are essentially independent of the numerical discretization.

3.2. Lagrangian method

In order to use Lagrangian method we need to know the time variations of the temperature of the gas element and the position of the gas element traveling inside the pulse tube with pressure oscillation. We will derive below the respective expressions. The general thermodynamic equations for real gas are given by

$$\mathrm{d}H_\mathrm{m} = T\,\mathrm{d}S_\mathrm{m} + V_\mathrm{m}\,\mathrm{d}p \tag{16}$$

$$\begin{aligned}\mathrm{d}H_\mathrm{m} &= C_\mathrm{P}\,\mathrm{d}T + \left\{V_\mathrm{m} - T\left(\frac{\partial V_\mathrm{m}}{\partial T}\right)_\mathrm{P}\right\}\mathrm{d}p \\ &= C_\mathrm{P}\,\mathrm{d}T + (1 - T\alpha_\mathrm{V})V_\mathrm{m}\,\mathrm{d}p,\end{aligned} \tag{17}$$

with α_V the volumetric thermal expansion coefficient

$$\alpha_\mathrm{V} = \frac{1}{V_\mathrm{m}}\left(\frac{\partial V_\mathrm{m}}{\partial T}\right)_\mathrm{P}. \tag{18}$$

Combining Eqs. (16) and (17) yields

$$T\,\mathrm{d}S_\mathrm{m} = C_\mathrm{P}\,\mathrm{d}T - T\alpha_\mathrm{V}V_\mathrm{m}\,\mathrm{d}p. \tag{19}$$

So we have

$$\left(\frac{\partial T}{\partial p}\right)_{S_\mathrm{m}} = \frac{1}{C_\mathrm{P}}\alpha_\mathrm{V}TV_\mathrm{m}. \tag{20}$$

In the adiabatic compression process the change of gas temperature related to the change of gas pressure can be expressed as

$$\frac{\mathrm{d}T}{\mathrm{d}t} \approx \left(\frac{\partial T}{\partial p}\right)_{S_\mathrm{m}}\frac{\mathrm{d}p}{\mathrm{d}t}. \tag{21}$$

Substituting Eq. (20) into Eq. (21) gives

$$\mathrm{d}T = \frac{1}{C_\mathrm{P}}\alpha_\mathrm{V}TV_\mathrm{m}\,\mathrm{d}p. \tag{22}$$

The temperature of the gas element with the pressure inside the tube is given by solving Eq. (22)

$$T = T^0 + \frac{1}{C_\mathrm{P}}\alpha_\mathrm{V}TV_\mathrm{m}(p - p^0). \tag{23}$$

The superscript 0 means variables at last time; variables without superscript stand for the value at present time.

In general, we have

$$T\,\mathrm{d}S_\mathrm{m} = C_\mathrm{V}\left(\frac{\partial T}{\partial p}\right)_{V_\mathrm{m}}\mathrm{d}p + C_\mathrm{P}\left(\frac{\partial T}{\partial V_\mathrm{m}}\right)_\mathrm{P}\mathrm{d}V_\mathrm{m}. \tag{24}$$

So

$$\left(\frac{\partial V_m}{\partial p}\right)_{S_m} = \frac{C_V}{C_P}\left(\frac{\partial V_m}{\partial p}\right)_T. \quad (25)$$

With the isothermal compression coefficient κ_T

$$\kappa_T = -\frac{1}{V_m}\left(\frac{\partial V_m}{\partial p}\right)_T, \quad (26)$$

Eq. (25) can be rewritten as

$$\left(\frac{\partial V_m}{\partial p}\right)_{S_m} = -\frac{C_V}{C_P}\kappa_T V_m. \quad (27)$$

The change of a volume V_t under adiabatic compressions is given by

$$\frac{dV_t}{dt} = \int_0^{L_t}\left(\frac{\partial V_m}{\partial p}\right)_{S_m}\frac{dp}{dt}\,dN = \frac{dp}{dt}\int_0^{L_t}\left(\frac{\partial V_m}{\partial p}\right)_{S_m}\frac{A_t}{V_m}\,dl. \quad (28)$$

Substituting Eq. (27) into Eq. (28) gives

$$\frac{dV_t}{dt} = -\frac{dp}{dt}\int_0^{L_t}\frac{C_V}{C_P}\kappa_T A_t\,dl. \quad (29)$$

Therefore the velocity of the gas element at cold end of the tube, related to the gas velocity at the hot end of the tube, is given by

$$u_L = u_H + \frac{dp}{dt}\int_0^{L_t}\frac{C_V}{C_P}\kappa_T\,dl. \quad (30)$$

The gas velocity at the hot end of the tube, can be calculated from the molar flow rate

$$u_H = \frac{n_H R T_H}{p_0 A_t}. \quad (31)$$

The position of gas element traveling with the pressure inside the pulse tube, leaving the hot heat exchanger at $x = L_t$ at a time $t = t_0$, is given by solving Eq. (30)

$$l = L_t - (p - p^0)\int_l^{L_i}\frac{C_V}{C_P}\kappa_T\,dx. \quad (32)$$

By using Eqs. (23) and (32) we can obtain the gas temperature profile and the position of the gas element traveling with pressure oscillations inside the pulse tube. Therefore, we can follow the tracks of gas particles in the pulse tube.

It should be noted that by using the Eulerian method it is impossible to obtain the explicitly analytical expression, like Eqs. (23) and (32), since Eqs. (1),(4)–(6) are non-linear and unsteady in Eulerian fixed grids. The temperature and the position (velocity) of the gas element have to be solved from an initial guess through an iterative scheme, as discussed in Section 3.1. Knowing the gas temperature profile and the position of the gas element traveling with pressure oscillations inside the pulse tube by using Lagrangian method, we can directly obtain the time variations of the gas and wall temperatures at the cold ends of first- and second-stage regenerators and the heat exchange rate (cooling power) in them. Then we use Eulerian methods, the fixed computational grids, to solve the variations of dynamic parameters in the regenerator through an iterative scheme.

4. Thermal properties of helium gas and regenerator materials

In the present simulation, the thermal properties of real helium gas, including density ρ (or molar volume V_m), heat capacity C_P, thermal conductivity k, viscosity η, volumetric thermal expansion coefficient α_V, and isothermal compression coefficient κ_T were obtained by the 32-term Jacobsen equation of state that is a modification of Benedict–Webb–Rubin equation of state [16]. The wide-ranging real thermal properties of helium of NIST TN-12 Helium Database were also obtained by using this equation. The density ρ_r, heat capacity C_r and thermal conductivity κ_r of the regenerator material were obtained by curve fitting.

5. Predicted results and discussions

A typical calculation is made for a two-stage PTC. The operating first stage temperature is 40 K, and the second stage is 4.2 K. The temperature of the hot-end heat exchanger is 300 K. The operating frequency is 1 Hz, and the mean pressure is 1.4 MPa. The main structure parameters are given in Table 1. The first-stage regenerator is filled with 250-mesh stainless steel screens, and its filling factor is 0.4. The second-stage regenerator is filled with lead spheres in 50% of the length and with Er_3Ni for 50% of the length, and its filling factor is 0.6.

The dynamic parameters, including gas temperature, pressure, mass flow rate and enthalpy flow, in the first- and second-stage regenerators during one cycle are shown in Fig. 2. The time variations of the gas temperatures, at the cold ends of the first-and second-stage regenerators during one cycle with the rotating valve angle are shown in Fig. 2(a). The amplitudes of the gas temperature fluctuation at the cold ends of the first- and second-stage regenerators are around 10 and 0.5 K, respectively. Much smaller fluctuation at the cold ends of the second-stage regenerators comes from the reason

Table 1
Main structure parameters of the two-stage PTC

Components	First stage	Second stage
Regenerator	∅60 mm × 140 mm	∅30 mm × 180 mm
Pulse tube	∅35 mm × 140 mm	∅18 mm × 330 mm
Buffer	1000 cm^3	1000 cm^3

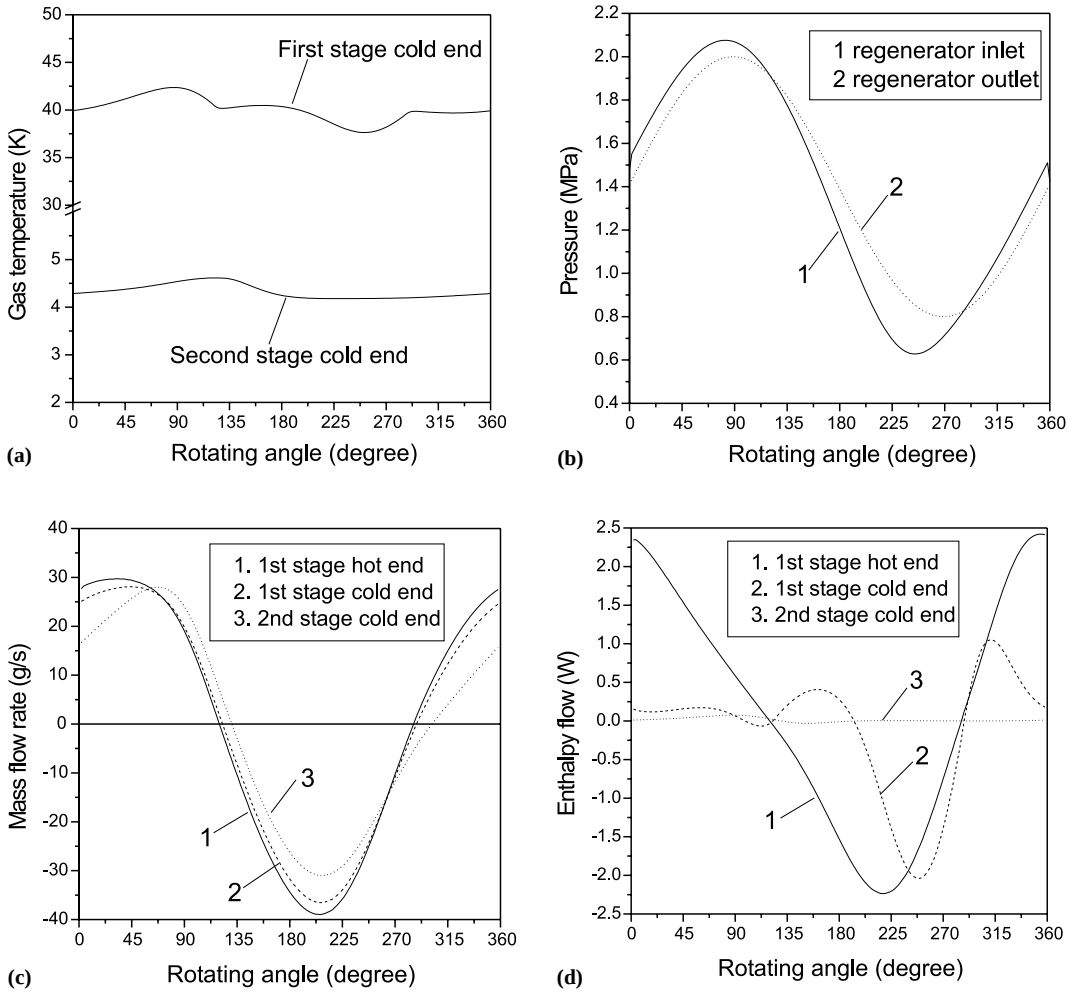

Fig. 2. Variations of dynamic parameters in one cycle: (a) temperature; (b) pressure; (c) mass flow rate; (d) enthalpy flow.

that the isothermal compressibility of helium is very small around 4.2 K. Fig. 2(b) gives the time variations of the dynamic pressures at the inlet and outlet of the first-stage regenerator during one cycle. There is 2–3 bar (non-linear) pressure drop across the first-stage regenerator, but nearly no pressure drop across the second-stage regenerator since the viscosity of the helium is much smaller at temperature range of 40–4.2 K than that of 300–40 K. The dynamic mass flow rate and the enthalpy flow at the first-stage hot end, the first-stage cold end and the second-stage cold end of the regenerators are plotted in Figs. 2(c) and (d), respectively.

Fig. 3(a) shows the average helium temperature distributions along the regenerator length, in the first- and second-stage regenerators. Fig. 3(b) shows the average helium temperature distributions along the second-stage regenerator. The monotonous, almost linear temperature distributions in the first-stage regenerator and non-linear temperature distributions in the second-stage regenerator were indicted, respectively.

Helium is generally used as the working gas for cryogenic cooler. Its thermal properties vary greatly in the low-temperature region (below 20 K), especially its density and specific heat capacity that increase greatly and have a sharp peak, as shown in Fig. 4. The specific heat capacity of stainless steel and lead, materials usually used in regenerators, decrease rapidly in the low-temperature region. Some magnetic materials have larger specific heat capacity below 10 K compared with common materials. However, it is impossible to cover the specific heat peak of helium using a single magnetic material. On the other hand, the different magnetic phase transitions of these magnetic materials with different temperature dependence of the specific heat allow the choice of optimal regenerative materials in form of multi-layered hybrid regenerator.

We will draw our attention here, to study and select the multi-layered hybrid regenerative materials in the second-stage regenerator to achieve larger cooling power and high performance for the 4 K PTC. It should be noted that the exact gas temperature profile inside the regenerator is a necessary condition for analyzing the multi-layered structure of the regenerative materials. The main structural parameters considered here are the

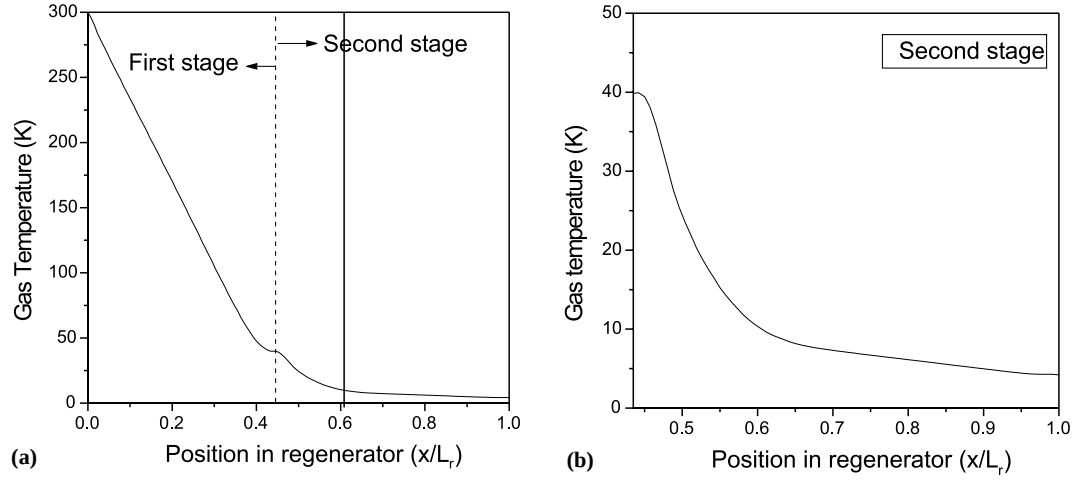

Fig. 3. Gas temperature profile inside regenerator: (a) first- and second-stage regenerator; (b) second-stage regenerator.

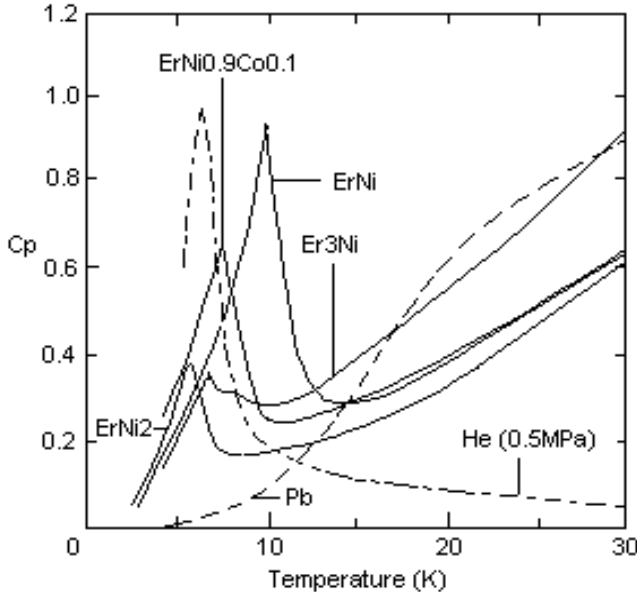

Fig. 4. Specific heat capacity of regenerator materials and helium.

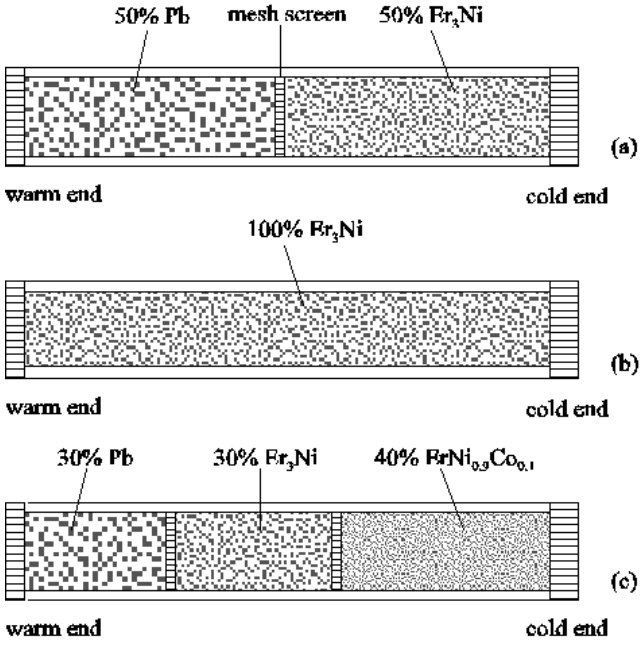

Fig. 5. Second-stage regenerator materials and arrangements.

same as shown in Table 1. The filling material in the first-stage regenerator is the same as above.

Below we will pay our attention to study and select the optimal regenerative materials in the second-stage regenerator to achieve larger cooling power for the cooler. We introduce a ratio ξ of specific heat capacity of the helium and matrix materials in regenerator in a cycle to judge the efficiency of the multi-layered hybrid regenerator:

$$\xi = \frac{(1-f)\rho C_{\mathrm{P}}}{f\rho_{\mathrm{r}} C_{\mathrm{r}}}. \tag{33}$$

Several different second-stage regenerator arrangements and materials were investigated in the simulation. Fig. 5 shows three typical types of regenerator arrangements and materials investigated in our numerical simulation.

Figs. 6(a) and (b) show the average specific heat capacity of regenerative materials along the first- and second-stage regenerators corresponding to the arrangements in Figs. 5(a) and (c), respectively. There are two salient protrusions along the regenerator in Fig. 6(a), which are caused by the strong increase of specific heat of lead and Er_3Ni. Similar features can be found in Fig. 6(b).

Figs. 7(a) and (b) give the time-averaged ratio ξ of specific heat of helium and regenerative materials along the first- and second-stage regenerators corresponding to the arrangements in Figs. 5(a) and (c), respectively. Very large values of ξ can be seen in the second-stage regenerator from 30% to 50% of the length (position

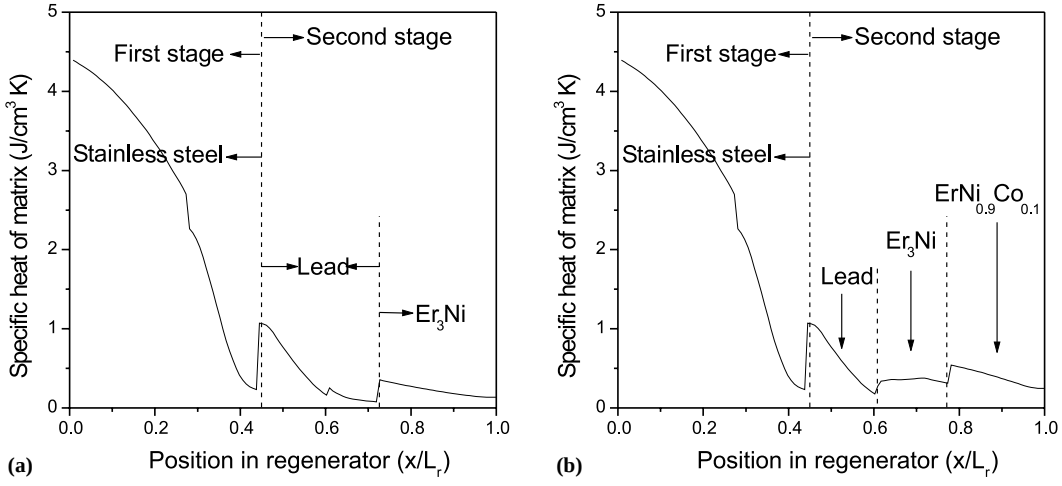

Fig. 6. Specific heat of regenerative materials inside the regenerator.

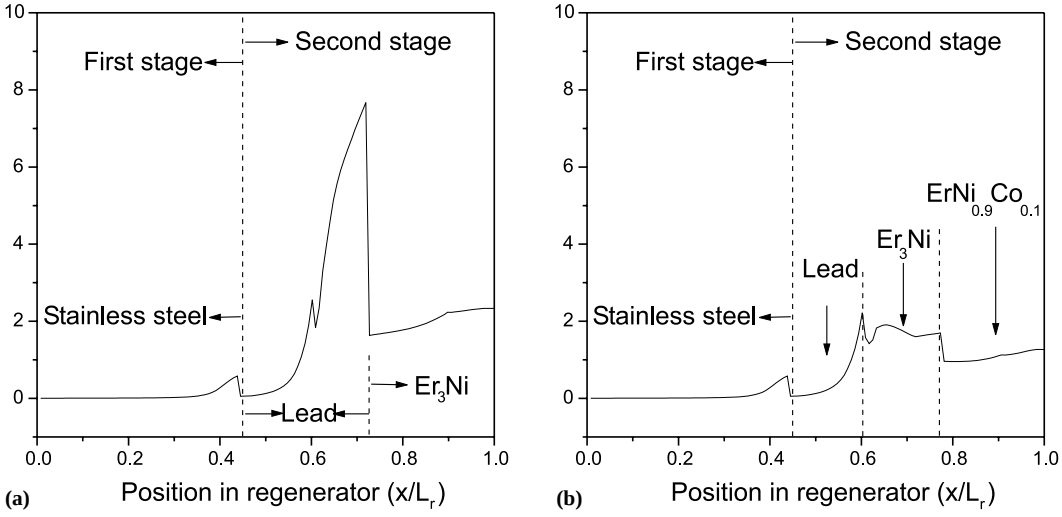

Fig. 7. Ratio of specific heat of helium and regenerative materials in the regenerator.

from 0.6 to 0.72 in Fig. 7(a)). This region of the second-stage regenerator is not efficient, demonstrating that lead in this section is not suitable as regenerative materials corresponding to the temperature profile inside the regenerator. In addition to this regenerative arrangement, predicting results of the case of Fig. 5(b) indicate that large values of ξ can be found in the section of the second-stage regenerator from 65% to the cold end of the length. This means that the Er_3Ni grain in this section of the regenerator is not suitable as regenerative material. Therefore, the regenerative materials and arrangements of Figs. 5(a) and (b) are not suitable in the 4 K two-stage PTC.

According to Fig. 4, we can see that the specific heat capacity of $ErNi_{0.9}Co_{0.1}$ below 10 K is larger than that of the other materials, although it is still smaller than that of helium. The large specific heat is helpful to improve the regenerator efficiency and heat exchange between the working gas and regenerative material, resulting in increasing the cooling capacity and lower the cooling temperature.

Comparing Fig. 7(b) with Fig. 7(a), as well as Fig. 6(b) with Fig. 6(a), we can find that the regenerative materials and arrangements of Fig 5(c) is more suitable for the 4 K PTC than that of Figs. 5(a) and (b). The predicted results of cooling power of the cooler also demonstrate that the arrangements of Fig. 5(c) can achieve larger cooling power than that of others, as shown in Fig. 8. So far, the optimum combinations of materials studied in the present simulation in second-stage regenerator were lead, Er_3Ni and $ErNi_{0.9}Co_{0.1}$. The optimum volumetric ratio of those three materials from hot end to the cold end of the regenerator were around 30%, 30% and 40%, as shown in Fig. 5(c). In this case, the predicted cooling power of the cooler is larger by about 0.2 W and 0.1 than the cases with regenerative

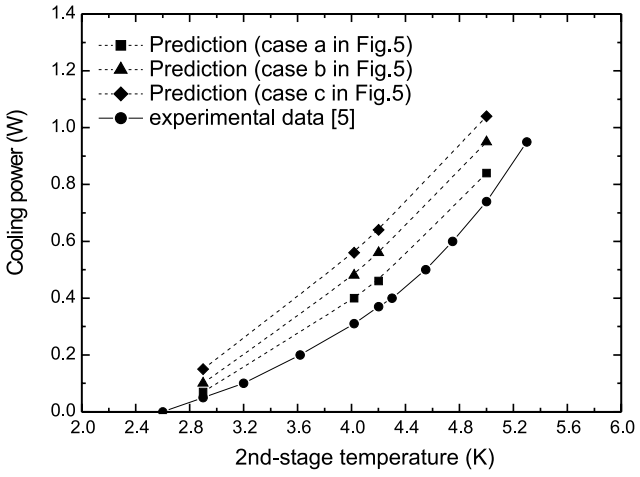

Fig. 8. The predicted cooling power versus cold-end temperature of the second-stage regenerator; the experiment data measured in [5] is also included.

arrangements of Figs. 5(a) and (b). It should be noted that the efficiency of multi-layered hybrid regenerative arrangements depends notably on the exact gas and matrix temperature profile along the regenerator.

Also, the prediction of the simulation is compared with the experimental results that include measurements of the temperature profile and the cooling power of second-stage regenerator. The best cooler performance was achieved with a three-layer structure of the second-stage regenerator matrix, filled with $ErNi_{0.9}Co_{0.1}$ grains in the lower 40%, Er_3Ni spheres in the middle 27% and lead spheres in the upper 33% of the regenerator length. The experimental regenerative arrangements were in good agreement with that of the numerical predictions. The predicted cooling power is about 35% higher than the experimental value (as shown in Fig. 8). The author reasons that the discrepancies can be attributed to the compressed heat generated inside the regenerator, additional heat losses due to radiation, DC gas flow through the double-inlet tube, transition to turbulence, which are not incorporated into the present numerical model.

6. Conclusions

A new mixed Eulerian–Lagrangian numerical model for simulating and visualizing the internal process and the variations of dynamic parameters of a two-stage PTC operating at 4 K temperature region has been developed. A variety of physical factors, such as real thermal properties of helium, multi-layered magnetic regenerative material, pressure drop and heat transfer in the regenerators, and heat exchangers, were taken into account in this model. Some predicted results of the time variation of the gas temperatures, the pressure, the mass flow rate and the enthalpy flow, in the first- and second-stage regenerators were presented in the paper. Attention was also paid to the effects of different regenerative materials on the performance of the two-stage PTC. The presented model can be used as an efficient tool for designing PTC operating at liquid helium temperature region.

Acknowledgements

The author would like to thank the members of Low Temperature Group, Eindhoven University of Technology, Netherlands, especially Professor A.T.A.M. de Waele, for many stimulating discussions.

References

[1] Radebaugh R. Recent developments of pulse tube refrigerators. In: Proceedings of the 19th International Conference on Refrigeration, vol. 3; 1995. p. 973.
[2] Radebaugh R. Advances in cryocoolers. Proc ICEC16/ICMC 1996;16:33.
[3] Matsubara Y, Gao J. Novel configuration of three-stage pulse tube cryocooler for temperatures below 4 K. Cryogenics 1994; 34:259.
[4] Chen GB, Qiu LM, et al. Experimental study on a double-orifice two-stage pulse tube refrigerator. Cryogenics 1997;37:271.
[5] Wang C, Thummes G, Heiden C. A two-stage pulse tube cooler operating below 4 K. Cryogenics 1997;37:159.
[6] Wang C, Thummes G, et al. Use of a two-stage pulse tube refrigerator for cryogen free operation of a superconducting Niobium–Tin magnet. Proc ICEC17 1998;17:69.
[7] Xu MY, de Waele ATAM, Ju YL. A pulse tube refrigerator below 2 K. Cryogenics 1999;39:865.
[8] Wang C. Numerical analysis 4 K of pulse tube coolers: Part I. Numerical simulation. Cryogenics 1997;37:207.
[9] Wang C. Numerical analysis of 4 K pulse tube coolers: Part II. Performance and internal processed. Cryogenics 1997;37:215.
[10] de Waele ATAM, Hooijkaas HWG, Steijaert PP, Benschop AA. Regenerator dynamics in the harmonic approximation. Cryogenics 1998;38:995.
[11] Ju YL, Wang C, Zhou Y. Numerical simulation and experimental verification of the oscillating flow in pulse tube cryocooler. Cryogenics 1998;38:169.
[12] Ju YL, Wang L, Zhou Y. Dynamic simulation of the oscillating flow with porous media in a pulse tube cryocooler. Numer Heat Transfer, Part A 1998;33:763.
[13] Steijaert PP. Thermodynamical aspects of pulse-tube refrigerators. Doctoral thesis, Eindhoven University of Technology, Netherlands; 1999.
[14] de Waele ATAM, Steijaert PP, Gijzen J. Thermodynamical aspects of pulse tube. Cryogenics 1997;37:313.
[15] Patanlar SV. Numerical heat transfer and fluid flow. New York: Hemisphere; 1980.
[16] McCarty RD, Arp VD. A new wide range equation of state for helium. Adv Cry Eng 1990;35:1465.